# Leukemic stem cell–niche interaction through CLEC2-podoplanin axis confers drug resistance in acute myeloid leukemia

Yoshio Iwata [1], Hirokazu Tanaka [1*], Takahiro Kumode [1], Hiroaki Inoue [1], Yasuyoshi Morita [1], Shinya Rai [1, 2], Itaru Matsumura [1]

[1] *Department of Hematology and Rheumatology, Kindai University Faculty of Medicine, Osaka, Japan*
[2] *Centre for Lymphoid Cancer, BC Cancer, Vancouver, BC, Canada*

## Abstract

**Background: Acute myeloid leukemia (AML) progression and therapy resistance are strongly influenced by the bone marrow microenvironment (BMME). Although recent genomic studies have advanced our understanding of AML pathogenesis, how leukemic stem cells (LSCs) adapt to and exploit niche interactions remains incompletely defined.**

**Methods: We established an in vivo–selected subline of the human AML cell line KG-1a by serial xenografting into NOD/SCID mice (rKG-1a). Phenotypic, transcriptional, and functional assays, including flow cytometry and cDNA microarray were performed. C-type lectin-like receptor 2 (CLEC2) expression in primary AML LSCs ($CD34^+CD38^-$) was assessed in 8 patient samples and these cells were co-cultured with stromal MS5 cells engineered to express podoplanin (Pdpn). Chemosensitivity was evaluated using cytarabine (Ara-C) and venetoclax (VEN).**

**Results: Compared with parental KG-1a, rKG-1a exhibited enhanced engraftment anaggressiveness *in vivo* despite slower proliferation *in vitro*. rKG-1a demonstrated downregulation of HLA class II and CD31, and upregulation of CD44, CD51, and CD62L. Microarray analysis identified CLEC2 as a top upregulated surface molecule, validated at both mRNA and protein levels. In patient-derived AML LSCs, CLEC2 expression was heterogeneous but significantly higher than in healthy HSCs. Functionally, $CLEC2^{high}$ LSCs displayed resistance to Ara-C when co-cultured with Pdpn-expressing stroma, whereas $CLEC2^{low}$ LSCs did not. Across 8 cases, $CLEC2^{high}$ status consistently associated with greater protection indices, although absolute CLEC2 intensity did not correlate linearly with chemoprotection.**

**Conclusions: Our findings establish CLEC2–Pdpn signaling as a novel axis of LSC–niche interaction that confers chemoresistance in AML. Targeting this pathway may provide therapeutic opportunities to eradicate resistant LSC subsets.**

**Key words: Acute myeloid leukemia, leukemic stem cells, bone marrow microenvironment, CLEC2, chemoresistance**

## 1. Background

Acute myeloid leukemia (AML) is a clonal hematopoietic malignancy arising from genetic and epigenetic alterations in hematopoietic stem or progenitor cells (HSPCs). Despite advances in intensive chemotherapy and the introduction of molecularly targeted therapies, long-term survival of AML patients remains dismal, particularly in older patients and those with relapsed/refractory disease [1-3]. Large-scale genomic studies have revealed recurrent driver mutations and provided important insights into leukemogenesis; however, mutational profiles alone cannot fully explain the clinical heterogeneity of AML in terms of treatment responses and relapse [4, 5]. Increasing attention has therefore turned to the bone marrow microenvironment (BMME), which critically influences AML progression as well as normal

Received September 26, 2025; Accepted October 15, 2025
DOI: 10.15100/0002004433

hematopoiesis [6-9].

BMME is composed of mesenchymal stromal cells, endothelial cells, osteolineage cells, adipocytes, immune subsets, and extracellular matrix components, together creating a dynamic ecosystem that regulates fate of hematopoietic stem cell (HSC) [10,11]. In AML, this microenvironment is profoundly remodeled, constituting a "malignant niche" that supports leukemic stem cells (LSCs) while impairing normal hematopoiesis[12-15]. Recent single-cell and spatial transcriptomic studies have revealed this altered stromal–immune cross-talk and niche compartmentalization in AML sustain AML cells and promote their resistance to therapy [16-18].

Several ligand–receptor interactions have been implicated in AML–niche crosstalk. The CXCL12–CXCR4 axis is one of the most extensively studied that mediates homing and retention of LSCs within protective niches and conferring resistance to cytarabine (Ara-C) [19-21]. Adhesion molecules such as VLA-4/VCAM-1, CD44/hyaluronic acid, and integrins reinforce these interactions and protect LSCs from chemotherapy-induced apoptosis [22, 23]. Additional signaling pathways including Notch, Wnt/β-catenin, and Hedgehog have also been implicated in LSC maintenance [24, 25]. Collectively, these studies highlight the concept that AML cells are not simply autonomous but dependent on reciprocal signaling within the BMME to survive and evolve.

Nevertheless, the spectrum of receptor–ligand pairs that mediate such protective interactions have not been fully defined, especially for those that are considered to regulate hemostasis and immunity. One such candidate is C-type lectin-like receptor 2 (CLEC2, also known as CLEC1B). CLEC2 is a platelet activation receptor that signals upon binding to its cognate ligand, podoplanin (Pdpn), a mucin-type glycoprotein expressed in lymphatic endothelial cells, fibroblasts, and bone marrow (BM) stromal cells [26, 27]. The CLEC2–Pdpn axis is essential for vascular development, platelet function, and immune regulation, and has more recently been implicated in HSC maintenance within the BM [28-31]. We previously reported that a subset of primitive HSCs expresses high levels of CLEC2, with enrichment of megakaryocyte/platelet gene programs, while intermediate progenitors downregulate CLEC2 expression and it is re-expressed at the megakaryocyte progenitor stage[32]. These observations suggested a lineage-associated regulatory role for CLEC2 within hematopoiesis. However, whether CLEC2 contributes to leukemogenesis or chemotherapy resistance in AML has remained unknown.

Based on these considerations, we hypothesized that CLEC2 expression on AML LSCs mediates protective interactions with Pdpn-expressing stromal cells in BMME, thereby conferring resistance to chemotherapy. To test this, we established an *in vivo*–selected aggressive AML model (rKG-1a), comprehensively profiled phenotypic and transcriptional changes, and validated the functional significance of CLEC2–Pdpn signaling in primary AML patient samples. Our findings identify CLEC2 as a novel therapeutic target and highlight the critical contribution of LSC–niche interactions in shaping drug resistance.

## 2. Patients and Methods

### 2.1. Patient samples

A total of 8 newly diagnosed AML patients were included in this study. This exploratory study was conducted using all eligible cases who provided written informed consent during the recruitment period (April 2023–March 2024), rather than based on a priori power calculation. Patients' characteristics are shown in Table 1. Diagnosis of these patients were defined by the WHO Classification 2017 and NCCN Guidelines Version 2.2025, respectively. Mononuclear cells were isolated from bone marrow (BM) samples. Normal healthy BM samples were obtained from patients with median age similar to AML patients, who did not have hematologic disease

Table 1

| case | Age | Sex | Dx | leukemic cell | karyotype | LC Surface phenotype |
|---|---|---|---|---|---|---|
| 1 | 74 | F | AML-MRC (M1) | 30% | +7, complex | CD34+33+13+ |
| 2 | 59 | M | AML-MRC | 30% | normal | CD34+33+13+ |
| 3 | 74 | F | AML-MRC | 55% | t(8;19) | CD34+33+13+7+ |
| 4 | 80 | M | AML-MRC | 99% | t(7;16) | CD34+33+13+7+ |
| 5 | 65 | M | AML-MRC | 20% | normal | CD34+33+13+ |
| 6 | 65 | F | AML (cup-like) | 100% | 4 | CD34+33+13+ |
| 7 | 55 | F | AML (M4) | 84% | normal | CD34+33+13+ |
| 8 | 68 | M | AML-MRC (M7) | 30% | complex | CD34+41+ |

as a result of the screening. Mononuclear cells were isolated with Ficoll-Paque PLUS (GE Healthcare Bio-Science AB, Uppsala, Sweden) and stored at Kindai University Faculty of Medicine until use. All samples were collected after obtaining the written informed consent from the patients. This study was approved by the ethics committee of our institute (Authorization Number: 24-017, 29-072) and conducted according to the Declaration of Helsinki.

**2.2. Cell lines and culture conditions**

The human AML cell line KG-1a was purchased from CLEA Japan, Inc. (Tokyo, Japan) and maintained in α-MEM medium (Thermo Fisher Scientific, Waltham, MA, USA) supplemented with 10% heat-inactivated fetal bovine serum (FBS; Sigma-Aldrich, St. Louis, MO, USA), 100 U/mL penicillin, and 100 μg/mL streptomycin at 37°C in a humidified atmosphere containing 5% $CO_2$. The murine stromal cell line MS5 was obtained from RIKEN Cell Bank (Tsukuba, Japan) and cultured in α-MEM supplemented with 10% FBS, 2 mM L-glutamine, and antibiotics as above.

**2.3. Retroviral transduction of stromal cells**

For Pdpn overexpression, full-length human Pdpn cDNA was cloned into a bicistronic retrovirus vector, pMSCV-IRES-DsRed gifted from Dr. Fujita J (Osaka University, Osaka, Japan). Retroviral particles were produced in a packaging cell line 293T containing the expression plasmids for gag and pol. MS5 cells were transduced with Pdpn or empty vector (Mock). Then, retrovirus-infected MS5 cells were isolated as DsRed-positive cells by FACS Aria (BD Biosciences, Franklin Lakes, NJ). Pdpn expression was also confirmed by flow cytometry using anti-human Pdpn antibody (Ab) (PDPN/1433; abcam, Cambridge, UK).

**2.4. Xenograft mouse model**

NOD.CB17-Prkdc$^{scid}$/Jcl (NOD/SCID) mice, aged 6–8 weeks, were purchased from Central Institute for Experimental Animals (Kawasaki, Kanagawa, Japan) and maintained under specific pathogen-free conditions. All animal experiments were approved by the Institutional Animal Care (approved ID: 06-13) and conducted in accordance with institutional guidelines. For primary transplantation, NOD/SCID mice were pretreated with 400 μL of phosphate-buffered saline containing 30 μL of anti-asialo GM1Ab (Wako, Osaka, Japan) 24 hours (hrs) before cell transplantation. The mice were injected with $1 \times 10^6$ KG-1a cells in 200 μL PBS intravenously via the tail vein 4 to 6 hrs after 200 cGy total body irradiation. After 6–8 weeks, BM cells were harvested from engrafted mice, and human $CD45^+$ cells were isolated by MACS using anti-human CD45 microbeads (Miltenyi Biotec, Bergisch Gladbach, Germany) to generate rKG-1a cells and cultured *in vitro* for 3 weeks. For secondary transplantation, $1 \times 10^6$ rKG-1a cells were injected into new NOD/SCID recipients, and mice were monitored for signs of leukemia. Leukemia onset was defined by ≥25% human $CD45^+$ cells in peripheral blood or clinical signs (lethargy, weight loss, and/or ruffled fur).

**2.5. Flow cytometry and cell sorting**

For patient-derived AML samples, mononuclear cells cells were stained with fluorochrome-conjugated Abs against human CD45 (HI30), CD34 (8G12), CD38 (HIT2), CD13 (WM15), CD33 (WM53), CD71 (L01.1), CD41 (HIP8), HLA-A (1082C5), HLA-B (YTH 76.3.rMAb), HLA-C (W6/32), HLA-DP (B7/21), HLA-DQ (Tu169), HLA-DR (L203.rMAb), CD31 (M89D3), CD44 (515), CD51 (RMV-7), CD62L (DREG-56) (all from BD Biosciences), and CLEC2 (AYP1, BioLegend, San Diego, CA or). Dead cells were excluded using propidium iodide or 7-AAD staining. Data acquisition was performed on a FACS Canto II (BD Biosciences), and analysis was carried out with FlowJo software (Tree Star, Ashland, OR, USA). LSCs were defined as $CD34^+CD38^-$cells. CLEC2 $^{high}$ and CLEC2 $^{low}$ fractions were sorted by FACS Aria as the top and bottom 30% of CLEC2 mean fluorescence intensity (MFI), respectively.

**2.6. Gene expression analysis**

RNA was extracted with PureLink® RNA Mini Kit (Thermo Fisher Scientific Inc.) according to the manufacturers' protocol. Gene expression analysis was conducted at Takara Bio Inc. (Shiga, Japan) using Agilent microarrays (https://catalog.takara-bio.co.jp/jutaku/?_fsi=hl3HYjFg&_fsi=hl3HYjFg&_fsi=hl3HYjFg). The gene expression profiling was performed on mRNA samples using SurePrint G3 Human GE v3 8x60K Microarray (Agilent Technologies, Santa Clara, USA) to compare the gene signatures between KG-1a and rKG-1a cells. Genes with an adjusted p-value < 0.05 and fold change > 2 were considered to be expressed with significant differences.

**2.7. Co-culture and drug sensitivity assays**

CLEC2 $^{high}$ or CLEC2 $^{low}$ LSC fractions ($1 \times 10^4$ cells/well) were co-cultured with confluent layers of MS5/Pdpn or MS5/Mock stromal cells in 96-well plates in StemSpan SFEM II medium (StemCell

Technologies, Vancouver, Canada) supplemented with 50 ng/mL stem cell factor (SCF), Flt3 ligand (FL), and thrombopoietin (TPO) (all from PeproTech, Thermo Fisher Scientific). Ara-C (0.1 μM or 0.5 μM) or venetoclax (VEN) (0.5 μM) (all from Selleck, Houston, TX ) was added for 48 hrs. Cell viability was determined by 7-AAD staining and flow cytometry. Viability was expressed as the percentage of 7-AAD $^-$ cells relative to untreated controls.

### 2.8. Evaluation of cell growth

For proliferation assays, KG-1a and rKG-1a cells were seeded into α-MEM medium with 10% FCS at an appropriate cell density ( $1 \times 10^4$ cells/mL) and cultured for the indicated times. Cell viability was measured with the Cell Titer Glo Reagent (Promega, Madison, WI) according to the manufacturer's recommendation using an Envision plate reader (Wallac, 1420 ARVO MX-2, Turku, Finland).

### 2.9. Data analysis and visualization

All statistical analyses and data visualization were performed using Python (v3.11). Data preprocessing and management were conducted with the pandas package. Statistical analyses included the Wilcoxon signed-rank test, Mann–Whitney U test, and Spearman correlation, performed using the scipy.stats module. Graphical outputs were generated using matplotlib and seaborn, including box-and-whisker plots, scatter plots with regression lines, volcano plots, and heatmaps. Linear regression lines were fitted with numpy.polyfit. Figures were assembled in Adobe Illustrator for final presentation.

### 2.10. Statistical analysis

All experiments were performed at least in biological triplicates unless otherwise specified. Experiments involving patient-derived primary AML cells, including CLEC2 expression analyses (Figure 4A, B), were performed once per patient sample due to limited cell availability. Data are presented as mean ± standard deviation (SD). Statistical analyses were conducted using GraphPad Prism 9 (GraphPad Software, La Jolla, CA, USA). Comparisons between two groups were done using the unpaired Student's t-test or Mann–Whitney U test, depending on data distribution. For multiple group comparisons, one-way ANOVA with Tukey's post-hoc test was used. Survival data were analyzed using the Kaplan–Meier method and compared by a log-rank test. A p-value < 0.05 was considered statistically significant.

## 3. Results

### 3.1 Establishment of a xenograft AML model and characterization of reconstituted KG-1a cells

To establish a human leukemia xenograft model, $1 \times 10^6$ KG-1a AML cells were intravenously injected into NOD/SCID mice pretreated with anti-asialo GM1 Ab to suppress NK cell activity and conditioned with lethal irradiation (Fig. S1). Leukemic engraftment was confirmed in BM and peripheral blood of all six transplanted mice (data not shown). In the primary transplantation cohort, mice survived up to 8 weeks before succumbing to progressive leukemia. BM cells harvested at week 10 was cultured *ex vivo* for three weeks under cytokine-free conditions, yielding rKG-1a cells (clone (cl) 1, 2 derived from separate mice) that had successfully engrafted *in vivo*.

Growth curves revealed that rKG-1a cells proliferated more slowly than the original KG-1a cells during the 7-day culture (Fig. 1A). Cell cycle analysis demonstrated the proportion of S and G2/M phases were reduced in rKG-1a cells compared with KG-1a cells (KG-1a 38.9 % *vs*. rKG-1a cl1 15.5 %, cl2 12.5 %), while the proportion of sub-G1 (indicative of apoptotic cell death fraction) was also lower in rKG-1a KG-1a 12.9 % *vs*. rKG-1a cl1 1.74 %, cl2 2.00 %), suggesting slowly growing and apoptosis-resistant phenotype of rKG-1a cells (Fig. 1B). Morphologically,

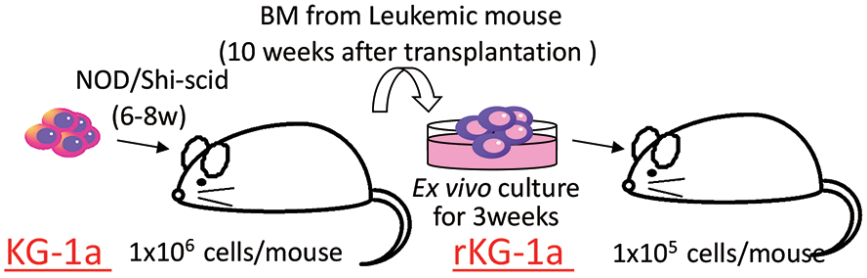


Fig. S1
Experimental schema of xenograft model generation. NOD/SCID mice were pretreated with anti-asialo GM1 antibody and lethal irradiation, followed by intravenous transplantation of $1 \times 10^6$ KG-1a cells. Bone marrow harvested 10 weeks post-transplantation was cultured under cytokine-free conditions for three weeks to generate rKG-1a cells.

both cl1 and cl2 of rKG-1a cells displayed distinct features from KG-1a cells with prominent nucleoli, reduced cytoplasm, and frequent cytoplasmic protrusions (Fig. 1C). When rKG-1a was transplanted into secondary recipients, leukemic engraftment was achieved with only $1 \times 10^5$ cells that are one tenth the number required for primary engraftment (data not shown). Moreover, rKG-1a-transplanted mice exhibited accelerated disease progression and earlier mortality compared with those receiving parental KG-1a (Fig. 1D). Together, these results demonstrate that *in vivo* passage selects for a leukemia subpopulation with enhanced malignant properties, characterized by improved engraftment *in vivo*, alongside slow cell cycling, reduced apoptosis, and unique morphological features *in vitro*.

### 3.2 Phenotypic analysis of rKG-1a cells reveals altered antigen presentation and adhesion molecule profiles

To further elucidate potential mechanisms underlying the enhanced engraftment and aggressiveness of rKG-1a cells, we next performed flow cytometric analysis of surface antigen expression,

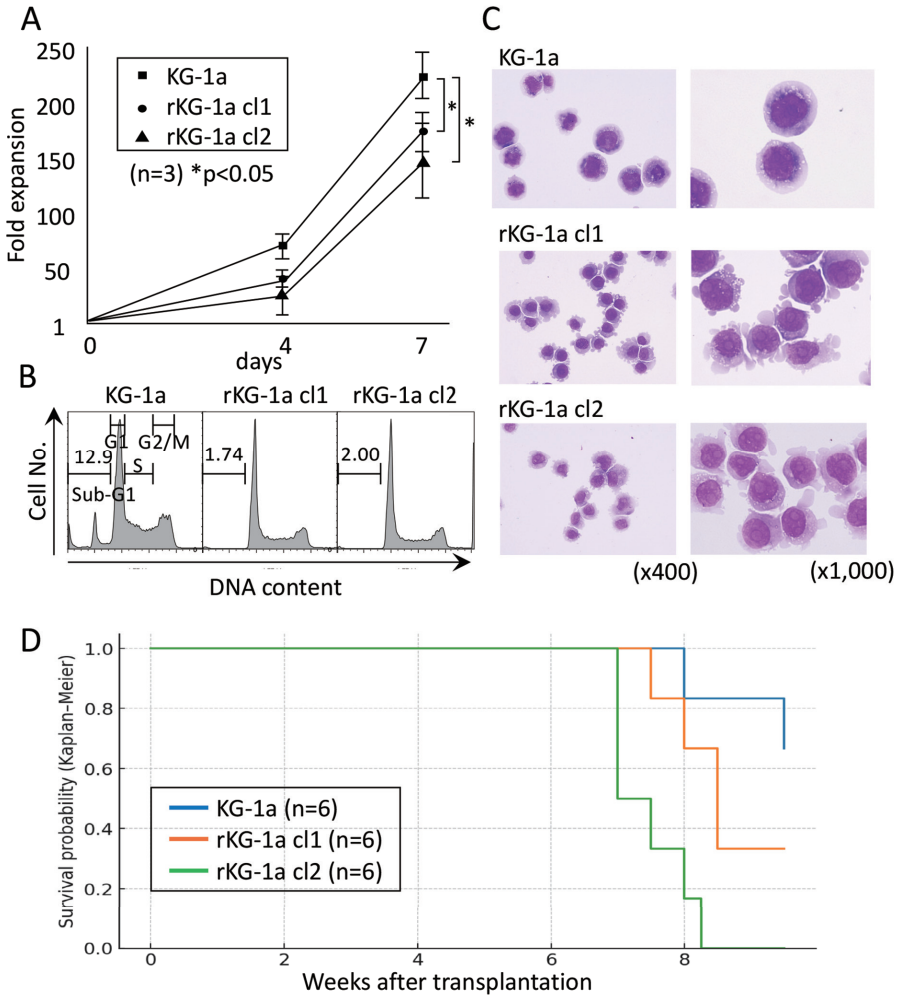


**Figure 1. Establishment of a xenograft AML model and characterization of rKG-1a cells.**

(A) Growth kinetics of KG-1a and rKG-1a *in vitro* over 7 days. rKG-1a displayed significantly reduced expansion compared with parental KG-1a (mean ± SD, n = 3; *p < 0.05).

(B) Cell cycle analysis of KG-1a and rKG-1a. rKG-1a contained fewer cells in S and G2/M phases, and exhibited a reduced sub-G1 fraction, suggesting attenuated cycling with decreased spontaneous apoptosis. Representative DNA content histograms are shown.

(C) Morphology of KG-1a and rKG-1a cells (May-Grunwald-Giemsa stain, ×400, ×1000). rKG-1a cells displayed prominent nucleoli, reduced cytoplasmic volume, and cytoplasmic protrusions, distinct from the morphology of parental KG-1a.

(D) Kaplan–Meier survival curves were generated for the three groups (KG-1a, rKG-1a cl1, and rKG-1a cl2). Transplantation with KG-1a resulted in survival up to 8 weeks (n = 6). The overall comparison using the log-rank test demonstrated a statistically significant difference among the groups ( $\chi^2 = 13.47$, df = 2, p = 0.0012).

focusing on immaturity/differentiation markers, activation markers, and adhesion molecules. Both KG-1a and rKG-1a were consistently positive for CD45 and CD34, with weak expression of CD133 and strong expression of CD13. Interestingly, CD33 was detectable in approximately half (41.1%) of KG-1a cells but hardly detectable in rKG-1a cells (cl1 0.7%; cl2 2.2%), indicating a loss of myeloid differentiation marker in rKG-1a cells (Fig. 2A). Moreover, the expression of CD38 and HLA-DR was severely reduced in rKG-1a cells, as well as a modest reduction in CD71 expression compared with parental KG-1a cells (Fig. 2A). Notably, the pronounced downregulation of HLA-DR raised the possibility of immune evasion by altered antigen presentation.

We therefore investigated in detail the expression of major histocompatibility complex (MHC) molecules, including class I HLA-A, -B, -C, and class II HLA-DP, -DQ, -DR, within the $CD34^{+}$ fraction. Flow cytometric analysis revealed that class I HLA expression was significantly higher in rKG-1a cells (~90%) than in KG-1a cells (~50%). In contrast, class II HLA expression, which was abundant in KG-1a (~90%), was almost completely absent in rKG-1a (Fig. 2B). This reciprocal alteration in HLA expression suggests a potential shift in the immune recognition profile of rKG-1a cells.

Because BMME plays a critical role in leukemic engraftment and survival, we also analyzed the expression of several adhesion molecules and chemokine receptors. Among the panel tested (CD31, CD44, CD49b, CD49d, CD49e, CD51, CD58, CD62E, CD62L, CD110, CD116, CD135, CXCR3, CXCR4, and CCR7), Compared with KG-1a cells, rKG-1a cells exhibited a striking reduction in CD31 expression, whereas the expression of CD44, CD51, and CD62L was increased (Fig. 2C). No apparent difference was observed in the expression of the other adhesion-related molecules between these cells (data not shown). These results suggest that rKG-1a cells not only alter the expression of molecules involved in immune responses but also modulate the expression of adhesion-related molecules, thereby enhancing their engraftment and leukemogenic potential in transplanted mice.

### 3.3 Identification of cell-surface functional molecules upregulated in rKG-1a by cDNA microarray, including CLEC2

To delineate the transcriptional basis of the phenotypic change observed in rKG-1a cells, we performed a two-color cDNA microarray (Cy3/Cy5 competitive hybridization) (Supplemental Table, which is available upon request due to its large size ). Among 5,599 probes, 308 transcripts were significantly altered in rKG-1a *vs*. KG-1a. Functional categorization highlighted pathways related to cell-cycle control, immune regulation/antigen presentation, and cell–cell/matrix adhesion (Fig. S2). Focusing on cell-surface molecules that may serve as therapeutic

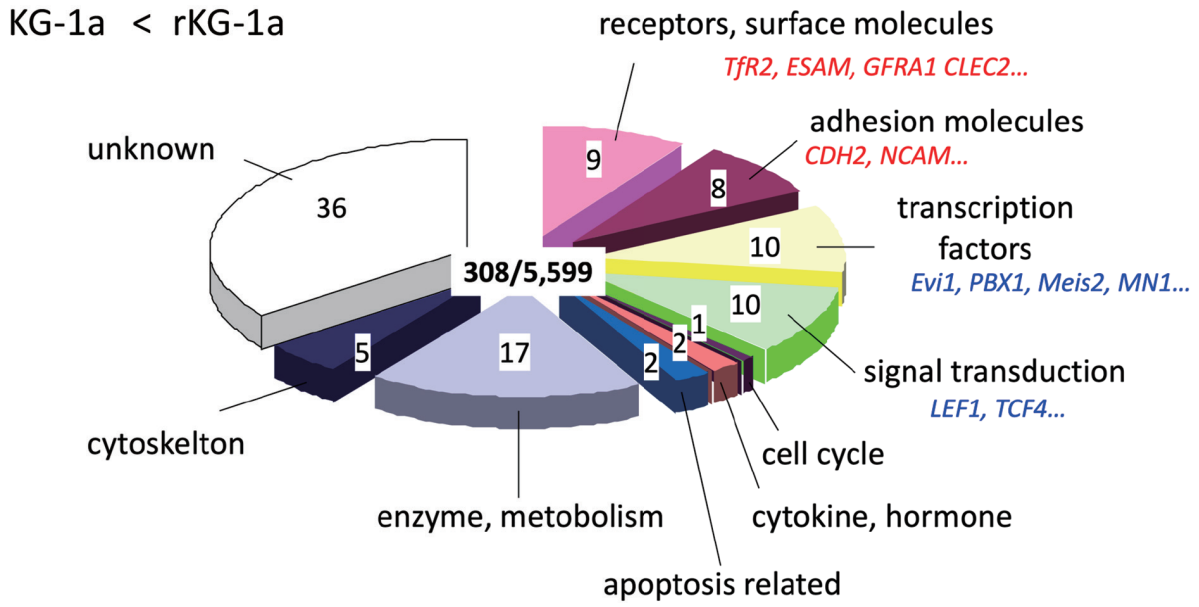


Fig. S2
Two-color cDNA microarray (Cy3/Cy5) comparing rKG-1a with KG-1a. Pie/bar plot shows functional categorization of the 308 significant transcripts among 5,599 assayed.

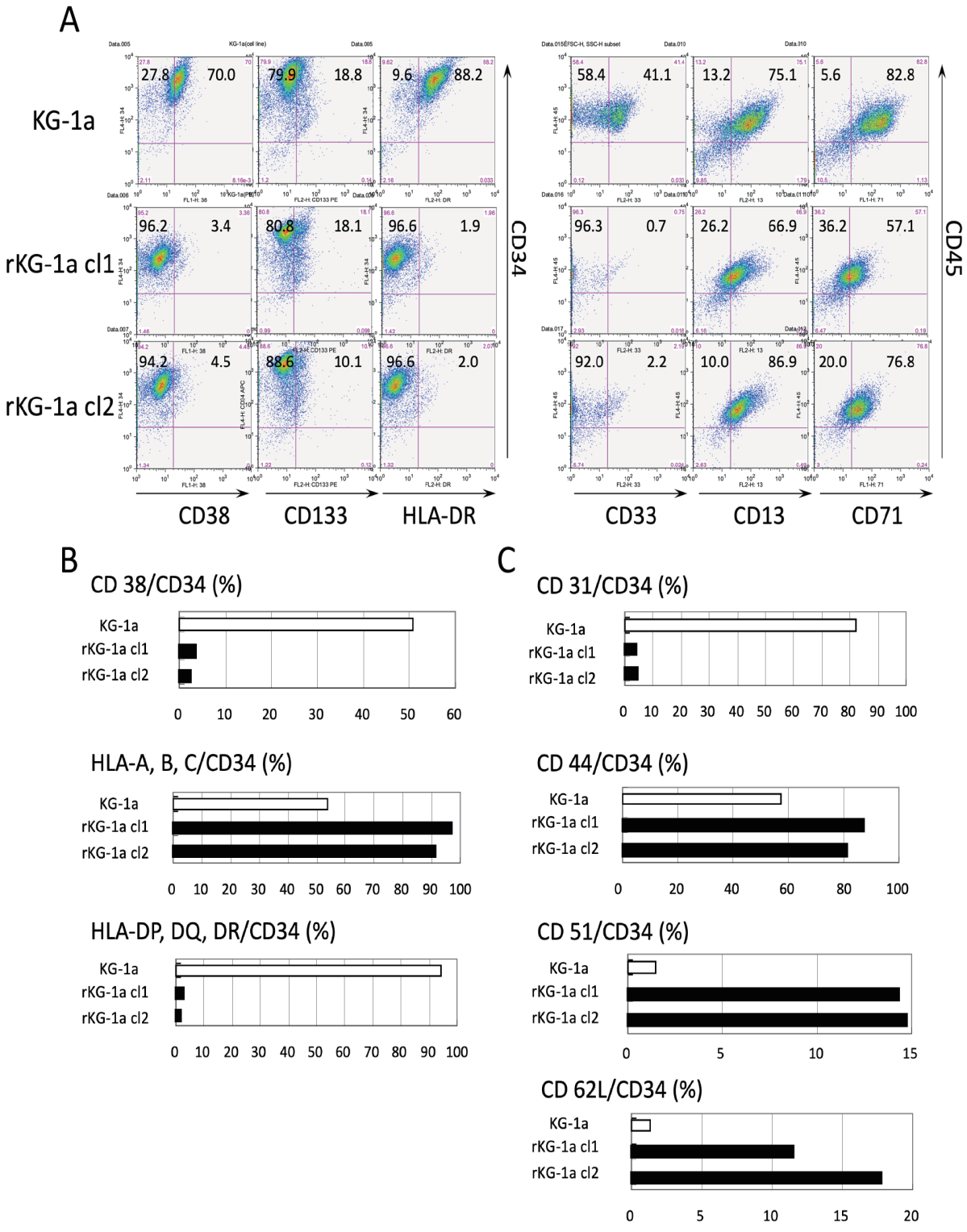


**Figure 2. Altered surface antigen and adhesion molecule profiles in rKG-1a cells compared with parental KG-1a cells.**

(A) Flow cytometric analysis of immaturity/differentiation markers (CD34, CD133/ CD13, CD33) and activation markers (CD38, HLA-DR, CD71) in KG-1a and rKG-1a cells. Representative histograms and quantification of positive fractions are shown. rKG-1a cells demonstrated loss of CD33 expression and marked reduction of CD38 and HLA-DR positivity.

(B) Differential expression of HLA molecules in $CD34^{+}$ fractions. Class I HLA (HLA-A, -B, -C) was upregulated in rKG-1a cells, whereas class II HLA (HLA-DP, -DQ, -DR) was almost completely lost compared with KG-1a cells.

(C) Expression of adhesion molecules and chemokine receptors in KG-1a and rKG-1a cells was evaluated with FCM. rKG-1a exhibited reduced CD31 but increased CD44, CD51, and CD62L expression.

targets, we ranked differentially expressed genes by the mean $\log_2$ fold-change across replicates and curated candidates using ontology/keyword filters (receptor/adhesion/lectin/transporter/channel, etc.). The top candidates included receptors (*e.g.*, NPR3, GFRA1), adhesion/axon-guidance molecules *(e.g.*, CDH2), ion channels, and receptor-type phosphatases (Fig. 3A). Importantly, among the upregulated surface molecules in rKG-1a, CLEC2 was selected for validation owing to its known expression in hematopoietic stem/progenitor cells (Ref. 32, as previously reported by our group) and its functional interaction with Pdpn within the bone marrow niche, which may contribute to LSC–stroma communication. Upregulation of CLEC2 was confirmed at the transcript level by qPCR and at the protein level by flow cytometry (Fig. 3B), supporting its candidacy as a niche-interactive therapeutic target.

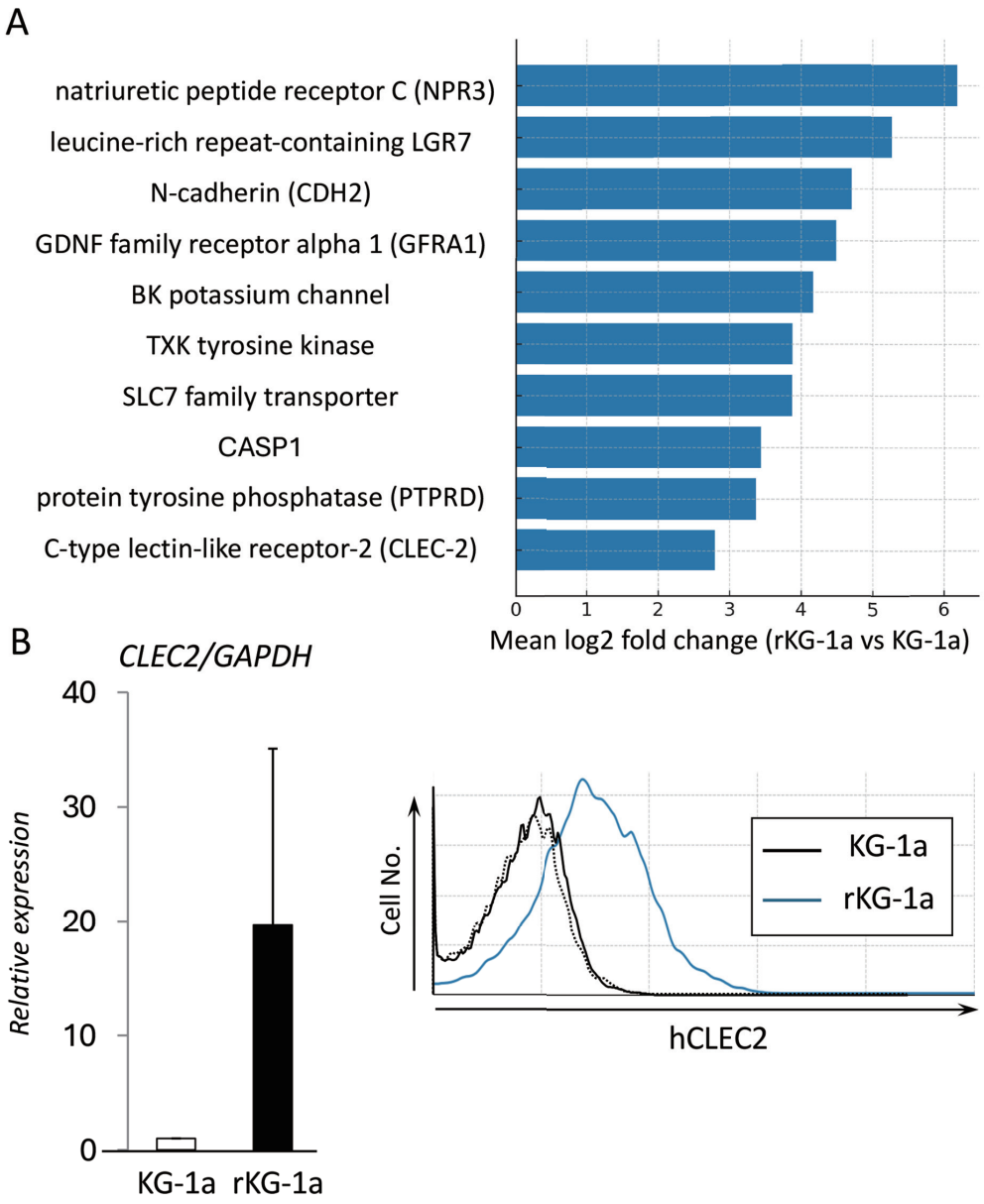


**Figure 3. Global transcriptional profiling identifies cell-surface functional molecules upregulated in rKG-1a, including CLEC2.**

(A) Ranked cell-surface functional molecules upregulated in rKG-1a based on mean $\log_2$ fold-change across replicates. Candidates were curated by ontology/keyword filters (receptors, adhesion molecules, channels, transporters, lectins).

(B) Validation of CLEC2 expression was evaluated by quantitative PCR (left panel) and flow cytometry (right panel). The blue and bock solid line indicate CLEC2 expression on rKG-1a and KG-1a, respectively, and the dotted line indicates the isotype control.

### 3.4 CLEC2-Pdpn interaction confers Ara-C resistance on CLEC2$^{high}$ LSCs.

We next compared CLEC2 expression in $CD34^+CD38^-$ fractions in AML samples (n=8) and healthy donors (HD) (n=8). Flow cytometric analysis revealed CLEC2 expression was significantly higher in $CD34^+CD38^-$ LSCs compared to normal $CD34^+CD38^-$ HSCs (Mann-Whitney U test, $p = 0.015$), whereas there was considerable variation in MFI among individuals within both the AML and HD groups (Fig. 4A). These findings suggest that CLEC2 expression marks a subset of LSCs in AML regardless of differentiation stages and cell lineages (Supplemental Table 1).

To investigate the functional impact of CLEC2 expression in primary LSCs, we employed a flow cytometry-based cell sorting strategy (Fig. 4B). After excluding dead cells with 7-AAD, $CD45^+CD34^+CD38^-$ LSCs were gated and subsequently stratified based on CLEC2 expression levels. As shown in Supplementary Fig. 3, CLEC2 expression levels varied considerably among AML cases, providing the basis for defining CLEC2$^{high}$ and CLEC2$^{low}$ subsets; accordingly, we defined the top 30% as CLEC2$^{high}$ and the bottom 30% as CLEC2$^{low}$ fractions. These samples were then used for functional assays.

To model interactions with the BM niche, we established stromal MS5 cells that stably express human podoplanin (MS5/Pdpn) using retroviral transduction, with empty vector-transduced cells (MS5/Mock) using as controls. Under physiological conditions, Pdpn is expressed by certain stromal and osteoblastic niche cells within the bone marrow, including reticular cells associated with hematopoietic stem cell maintenance [33]. This supports the relevance of Pdpn-mediated interactions in our co-culture model. CLEC2$^{high}$ and CLEC2$^{low}$ LSCs derived from Case 1 (AML-MRC) were co-cultured with either MS5/Pdpn or MS5/Mock under serum-free conditions, supplemented with cytokines (SCF, TPO, and FL, each at 50 ng/mL). The sensitivity of these LSCs to Ara-C, a key chemotherapeutic agent for AML, or VEN, a BCL-2 inhibitor known to improve clinical outcomes in newly diagnosed, relapsed and refractory AML [2, 3], was then evaluated. In the absence of Ara-C, approximately 10% of cells underwent cell death ($CD45^+$7-$AAD^+$) after 48 hrs of co-culture, regardless of CLEC2 expression status (Fig. 4C).

Upon exposure to 0.1 μM Ara-C, co-culture with MS5/Mock increased the fraction of dead cells to approximately 50%, with a more pronounced, but not statistically significant, effect observed in CLEC2$^{low}$ LSCs (48.2 ± 7.3% vs. 55.9 ± 11.3%, p=0.08) (Fig. 4C, 4D). Notably, co-culture with MS5/Pdpn significantly attenuated Ara-C-induced cytotoxicity in CLEC2$^{high}$ LSCs (48.2 ± 7.3% vs. 30.4 ± 2.1%, $p<0.05$). In contrast, no protective effect was observed in CLEC2$^{low}$ cells (55.9 ± 11.3% vs. 54.7 ± 3.6%, p=0.90) (Fig. 4C, 4D left panel). These results indicate that the CLEC2-Pdpn interaction selectively promotes chemoresistance in CLEC2$^{high}$ LSCs. Similarly, when VEN (0.5 μM) was added, co-culture with MS5/Pdpn significantly reduced cytotoxicity in CLEC2$^{high}$ LSCs compared with co-culture with MS5/Mock (49.9 ± 5.4% vs. 39.1 ± 5.8%, $p < 0.05$), whereas no such effect was observed in CLEC2$^{low}$ LSCs (31.9 ± 12.7% vs. 40.6 ± 1.0%, $p = 0.51$) (Fig. 4C, 4D, right panel).

### 3.5 Patient-level aggregation: protection indices by CLEC2 status and pharmacologic condition

To determine whether Pdpn, expressed in stromal cells, confers significant protective effects against Ara-C in CLEC2$^{high}$ LSC populations in additional AML patients, we quantified its effect using a protection index (PI), defined as PI = 1 - (cell death rate (%) in Pdpn / cell death rate (%) in Mock). In CLEC2$^{high}$ LSCs, Pdpn significantly reduced Ara-C-induced cytotoxicity at both 0.1 and 0.5 μM (median PI 0.226 [0.114–0.271], $p = 0.0117$; 0.243 [0.156–0.321], $p = 0.0156$; one-sided Wilcoxon vs 1). In CLEC2$^{low}$ fractions, evidence of protection was limited (0.1 μM: median PI 0.044 [−0.061–0.204], $p = 0.313$) (Fig.5A).

We also examined PI under VEN (0.5 μM) treatment. However, the results were inconclusive due to the limited sample size (CLEC2$^{high}$ median PI 0.103, $p = 0.109$; CLEC2$^{low}$ median PI 0.220, $p = 0.125$) (Fig.5B). These data indicate that CLEC2-Pdpn signaling preferentially mediates Ara-C resistance in CLEC2$^{high}$ LSCs.

### 3.6 Absolute CLEC2 intensity does not linearly predict chemoprotection across patients

Finally, we investigated whether absolute intensity of CLEC2 expression (measured as MFI in the CLEC2$^{high}$ fraction) correlated with the degree of Pdpn-mediated chemoprotection. In eight AML patients, no significant correlation was observed under treatment with Ara-C (0.1 μM: $\rho = -0.48$, $p = 0.24$; 0.5 μM: $\rho = 0.26$, $p = 0.62$) or VEN (0.5 μM: $\rho = 0.07$, $p = 0.91$) (Fig. 5B, S3). These results suggest that the presence of CLEC2$^{high}$ cells, rather than the absolute MFI level, is more relevant to the chemoprotective phenotype. This finding indicates that the qualitative presence of CLEC2$^{high}$ LSC subsets, rather than quantitative differences in surface

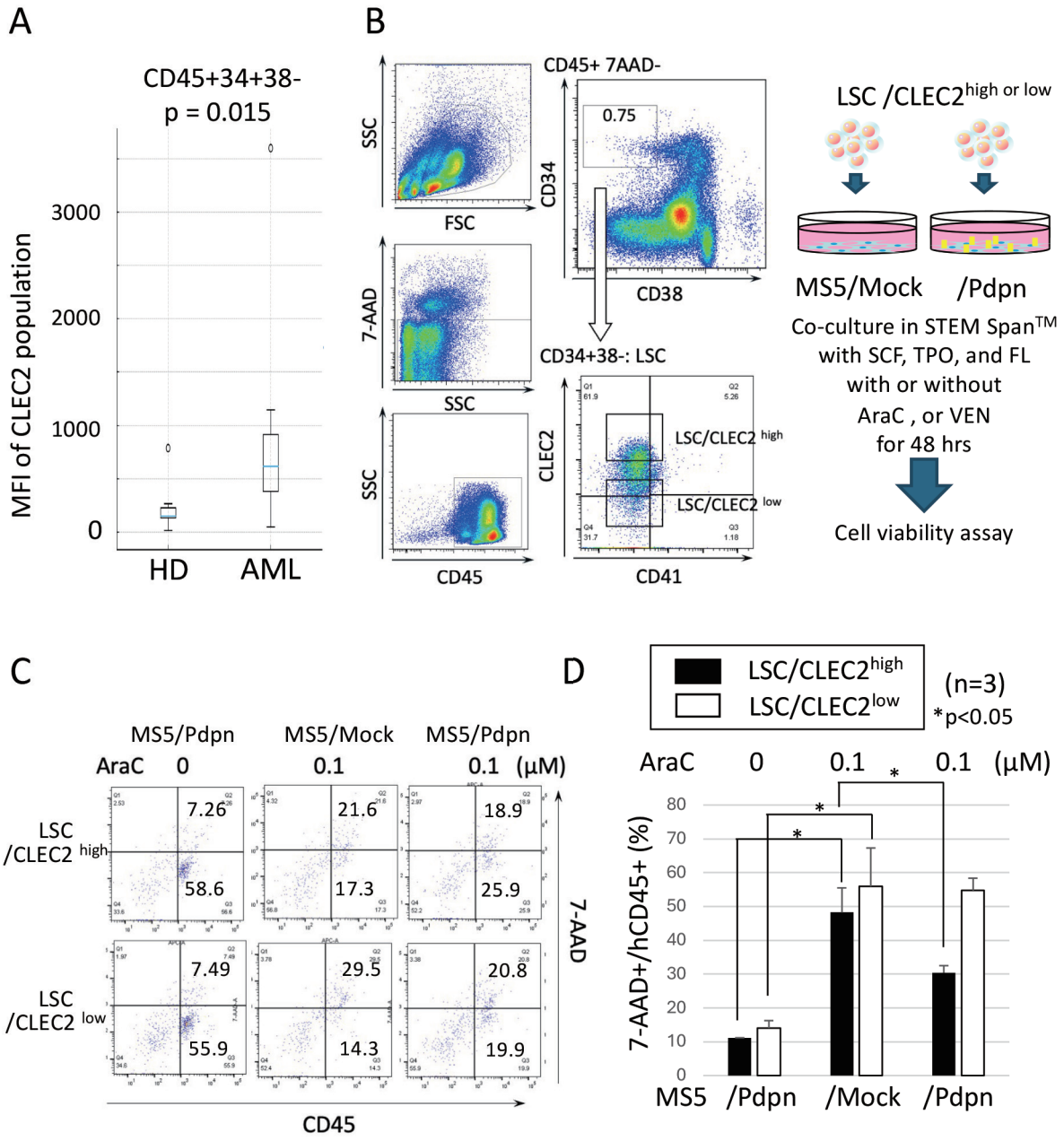


**Figure 4. CLEC2/Pdpn interaction confers Ara-C resistance in CLEC2$^{high}$ leukemic stem cells.**

(A) Box-and-whisker plots of CLEC2 mean fluorescence intensity (MFI) in leukemic stem cell fractions ($CD45^+CD34^+CD38^-$) from AML patients (n=8) and in hematopoietic stem/progenitor cell fractions from healthy donors (n=8). Boxes represent the interquartile range (IQR), horizontal lines indicate the median, and whiskers show the range. Statistical significance was assessed using the Mann-Whitney U test (p = 0.015).

(B) Representative gating strategy for the isolation of LSCs. Dead cells were excluded by 7-AAD staining, followed by gating of $CD45^+$ $CD34^+$ $CD38^-$ fractions, and further separation according to CLEC2 (and CD41) expression. CLEC2$^{high}$ (top 30% MFI) and CLEC2$^{low}$ (bottom 30% MFI) populations were used for downstream assays. Fig.4B right panel is shown experimental scheme of co-culture. CLEC2$^{high}$ and CLEC2$^{low}$ LSCs were co-cultured with stromal cell lines expressing podoplanin (MS5/Pdpn) or empty vector controls (MS5/Mock) in cytokine-supplemented serum-free medium, with or without Ara-C (0.1, 0.5 $\mu$M) or VEN (0.5 $\mu$M) for 48 hours (hrs).

(C) Representative flow cytometric analyses after 48 hrs of co-culture. The left panel shows cultures with Ara-C (0.1 $\mu$M) and the right panel shows cultures with VEN (0.5 $\mu$M). Cells were plotted with CD45 on the x-axis and 7-AAD on the y-axis, and the percentages of cells within each quadrant are indicated.

(D) Quantification of cell death ($CD45^+$ $7\text{-}AAD^+$) after co-culture with LSC derived from Case 1. While MS5/Mock failed to protect LSCs from Ara-C- or VEN-induced cytotoxicity, MS5/Pdpn provided significant resistance specifically to CLEC2$^{high}$ LSCs ($p<0.05$). Data represent mean ± SD (n=3).

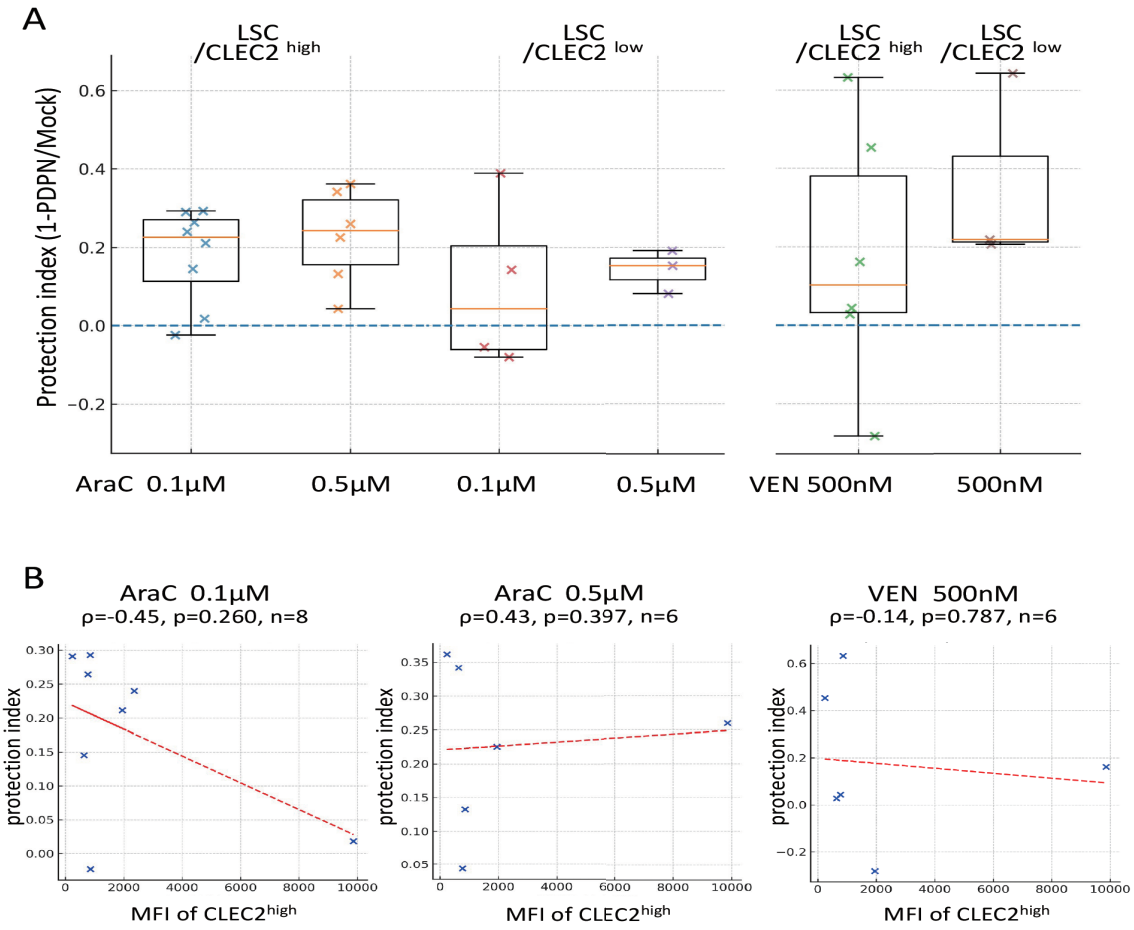


**Figure 5. Clinical correlation of CLEC2 expression with chemoprotection.**

(A) Protection index of primary AML LSCs stratified by CLEC2 status (CLEC2$^{high}$ vs CLEC2$^{low}$) under Ara-C (0.1 $\mu$M, 0.5 $\mu$M) and VEN (0.5 $\mu$M) treatment. Data are shown as box-and-whisker plots with each dot representing an individual case (n=6-8). CLEC2$^{high}$ LSCs tended to exhibit higher protection under Pdpn co-culture compared with CLEC2$^{low}$ LSCs, although statistical significance varied by condition.

(B) Scatter plots showing correlation between expression level of CLEC2 MFI and protection index under (left panel) Ara-C 0.1 $\mu$M, (middle panel) Ara-C 0.5 $\mu$M, and (right panel) VEN 0.5 $\mu$M. Spearman correlation coefficients ($\rho$) and p values are indicated. No significant correlation was observed, suggesting that absolute expression intensity does not directly determine chemoresistance.

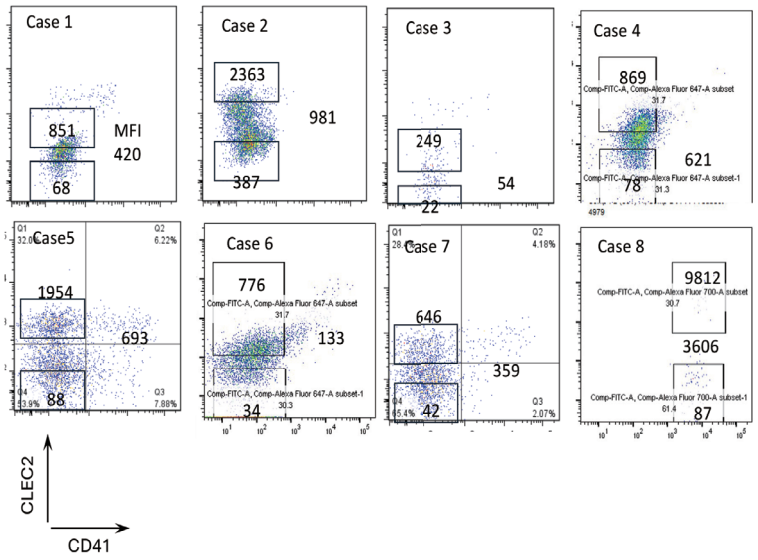


**Fig. S3**

Distribution of CLEC2 mean fluorescence intensity (MFI) across the eight AML cases is shown, demonstrating inter-patient variability in expression levels. Based on these data, CLEC2$^{high}$ and CLEC2$^{low}$ populations were defined according to CLEC2 MFI, with the top 30% designated as CLEC2$^{high}$ and the bottom 30% as CLEC2$^{low}$.

expression intensity, likely underlies the observed chemoprotective effect.

## 4. Discussion

In this study, we identified CLEC2 as a molecule upregulated in AML cells with enhanced leukemogenic potential in a xenograft model. CLEC2 was variably expressed in primary AML LSCs, and its interaction with stromal Pdpn conferred marked resistance to chemotherapy, including Ara-C and VEN. These findings extend the repertoire of known BMME–LSC interactions, such as VLA-4/VCAM-1, CD44/hyaluronan, and CXCL12/CXCR4 [19-23]—to now include the CLEC2–Pdpn axis as a novel mechanism of niche-mediated drug resistance in AML.

The altered immunophenotype observed in rKG-1a cells—marked by downregulation of HLA-class II and CD31 alongside upregulation of CD44, CD51, and CD62L—suggests a broader remodeling of adhesion and immune recognition pathways during leukemia progression. CLEC2 upregulation should be regarded as one element within this broader set of changes, and these alterations may represent parallel or context-dependent adaptations induced by the xenograft environment. However, several limitations of this study should be acknowledged. As mentioned above, our findings are based on an artificial xenograft model, and whether the same mechanisms operate in human AML *in vivo* remains uncertain. In particular, we were unable to assess the expression pattern of Pdpn within the native bone marrow niche, leaving the physiologic relevance of the CLEC2–Pdpn axis incompletely defined. Moreover, although rKG-1a cells consistently exhibited alterations in adhesion molecules, it remains unresolved whether these changes are downstream of CLEC2–Pdpn signaling or parallel consequences of xenograft-driven adaptation. Notably, in our patient cohort, absolute CLEC2 expression levels (MFI) did not correlate with protection indices against Ara-C or VEN, indicating that CLEC2 intensity alone is not a sufficient predictor of chemoresistance. Although this finding is negative, it provides important insights: CLEC2 requires the appropriate microenvironmental context—most notably stromal Pdpn—to exert its protective effect. It also implies that inter-patient heterogeneity in drug resistance is likely shaped by the complex interplay of multiple adhesion and signaling pathways, rather than by CLEC2 expression alone.

Although not directly tested in this study, CLEC2 has been shown to signal through the Syk kinase pathway in platelets and megakaryocytes [34, 35]. This raises the possibility that CLEC2–Syk signaling may also operate in AML LSCs, modulating adhesion phenotypes and contributing to drug resistance. If validated, this would link the observed phenotypic remodeling to a defined molecular pathway and position Syk inhibitors—already in clinical use for other hematologic malignancies—as promising therapeutics in CLEC2$^{high}$ AML.

Our previous work demonstrated that a subset of human HSCs with high CLEC2 expression shows a megakaryocyte/platelet-biased transcriptional program, with CLEC2 expression being repressed during early myeloid differentiation but reappearing in MkPs [32]. The finding that CLEC2$^{high}$ AML LSCs are preferentially chemoresistant raises the intriguing possibility that megakaryocyte lineage-biased progenitors may be inherently more niche-dependent and drug-resistant, and that AML evolution exploits this lineage program. Similar lineage biases have been reported in normal hematopoiesis and may be co-opted in leukemogenesis.

From a therapeutic perspective, the CLEC2–Pdpn axis is attractive for several reasons. CLEC2 expression in normal hematopoiesis is largely restricted to megakaryocytes and platelets, implying limited off-target toxicity if CLEC2 is targeted on LSCs. Abs or small molecules disrupting CLEC2–Pdpn interactions could abrogate LSC adhesion to protective niches without severely impacting normal HSC maintenance. In addition, Syk inhibitors might attenuate CLEC2-driven signaling downstream, potentially reversing drug resistance. In addition, while CLEC2 expression alone did not correlate with chemoprotection in our cohort, its evaluation in combination with other niche- or lineage-associated markers may contribute to a stratification framework for identifying AML subtypes with distinct microenvironmental dependencies. From a translational perspective, targeting the CLEC2–Pdpn axis represents a promising therapeutic approach. Potential strategies include blocking CLEC2–Pdpn binding or inhibiting downstream SYK signaling. Given the physiological expression of CLEC2 in megakaryocytes and platelets, off-target effects on hemostasis should be carefully assessed in future studies.

## 5. Conclusion

Our findings identify CLEC2 as a key determinant of LSC–niche interactions in AML. Targeting the CLEC2–Pdpn axis, either directly or through downstream pathways such as Syk, may represent a rational strategy to sensitize resistant LSCs to chemotherapy.

Data Availability Statement:

The data presented in this study are available upon request from the corresponding author.

Acknowledgments:

The authors thanks Keiko Furukawa and Ayumi Nakamura for technical help, Shinji Kurashimo for assistance with flow cytometric studies and all staff at Department of Hematology and Rheumatology, the Kindai University Faculty of Medicine.

Conflicts of Interest:

H. Tanaka received grants from JSPS KAKENHI, ONO PHARMACEUTICAL CO., LTD., and Kyowa Kirin Co., Ltd.; personal fees from Bristol-Myers Squibb (Celgene), Novartis Pharmaceuticals, Janssen Pharmaceutical K.K, Sanofi, and Meiji Seika Pharma Co., Ltd..

T. Kumode received personal fees from ONO PHARMACEUTICAL CO., LTD., Janssen Pharmaceutical K.K, AbbVie GK, BeiGene, Ltd., AstraZeneca PLC, and Genmab A/S.

K. Serizawa received personal fees from Janssen Pharmaceutical K.K, Takeda Pharmaceutical Company Limited, and Sanofi.

Y. Morita received personal fees from AbbVie GK, NIPPON SHINYAKU CO., LTD., and Alexion Pharmaceuticals, Inc.

H. Hanamoto received personal fees from Pfizer Japan Inc., CSL Behring, and Takeda Pharmaceutical Company Limited.

I. Matsumura received grants from ONO PHARMACEUTICAL CO., LTD., NIPPON SHINYAKU CO., LTD., Kyowa Kirin Co., Ltd., Sumitomo Dainippon Pharma Co., Ltd., Shionogi & Co., Ltd., TEIJIN PHARMA LIMITED., Boehringer Ingelheim, Sanofi, Chugai Pharmaceutical Co., Ltd., Eisai Co., Ltd., MSD K.K, ASAHI KASEI PHARMA CORPORATION, Astellas Pharma Inc., Takeda Pharmaceutical Company Limited., Japan Blood Products Organization, NIHON PHARMACEUTICAL CO., LTD, DAIICHI SANKYO COMPANY, TAIHO PHARMACEUTICAL CO., LTD., Mitsubishi Tanabe Pharma Corporation, Nippon Kayaku Co.,Ltd., CSL Behring, Mundipharma K.K, AYUMI Pharmaceutical Corporation, Eli Lilly Japan K.K., and Actelion Pharmaceuticals Japan Ltd.,; personal fees from Bristol-Myers Squibb (Celgene), Novartis Pharmaceuticals, ONO PHARMACEUTICAL CO., LTD., Janssen Pharmaceutical K.K, NIPPON SHINYAKU CO.,LTD., Shionogi & Co., Ltd., Astellas Pharma Inc., Takeda Pharmaceutical Company Limited., DAIICHI SANKYO COMPANY, AbbVie GK, and Amgen BioPharma K.K. The remaining authors declare no competing financial interests.

The remaining authors declare no competing financial interests.

Funding:

The authors declare that this study received funding from JSPS KAKENHI Grant Number 23K07846. The funder was not involved in the study design, collection, analysis, interpretation of data, the writing of this article or the decision to submit it for publication.

## References

1. Papaemmanuil E, et al. (2016) Genomic classification and prognosis in acute myeloid leukemia. N Engl J Med, 374(23), 2209-2221
2. Döhner H, et al. (2015) Acute Myeloid Leukemia. N Engl J Med, 373 (12), 1136-1152
3. Estey EH. (2020) Acute myeloid leukemia: 2021 update on risk-stratification and management. Am J Hematol, 95(11), 1368-1398
4. Haferlach T, et al. (2014) Landscape of genetic lesions in 944 patients with myelodysplastic syndromes. Leukemia, 28(2), 241-247
5. Jones MF, et al. (2024) Mechanisms of Resistance to Targeted Therapies in AML Annu Rev Cancer Biol, 8, 81-96
6. Schepers K, et al. (2015) Bone marrow niches: a blueprint for regeneration and leukemia. Haematologica, 100(5), 515-525
7. Kumar B, et al. (2018) Acute myeloid leukemia transforms the bone marrow niche into a leukemia-permissive microenvironment. Leukemia, 32(3), 575-587
8. Schepers K, et al. (2015) Normal and leukemic stem cell niches: insights and therapeutic opportunities. Cell Stem Cell, 16(3), 254-267
9. Méndez-Ferrer S, et al. (2020) Bone marrow niches in haematological malignancies. Nat Rev Cancer, 20(5), 285-298
10. Morrison SJ, et al. (2014) The bone marrow niche for haematopoietic stem cells. Nature, 505(7483), 327-334
11. Crane GM, et al. (2017) Adult haematopoietic stem cell niches. Nat Rev Immunol, 17(9), 573-590
12. Hanoun M, et al. (2014) Acute myelogenous leukemia-induced sympathetic neuropathy promotes malignancy in an altered hematopoietic stem cell niche. Cell Stem Cell, 15(3), 365-375
13. Boyd AL, et al. (2017) Acute myeloid leukaemia disrupts endogenous myelo-erythropoiesis by compromising the adipocyte bone marrow niche.

Nat Cell Biol, 19(11), 1336-1347
14. Friedmann R, et al. (2023) Microenvironment and therapy-resistance in leukemias. Front Oncol, 13, 1244642
15. Bakhtiyari M, (2023) The role of bone marrow microenvironment (BMM) cells in acute myeloid leukemia (AML) progression: immune checkpoints, metabolic checkpoints, and signaling pathways. Cell Commun Signal, 21(1), 252
16. Baryawno N, et al. (2019;) A cellular taxonomy of the bone marrow stroma in homeostasis and leukemia. Cell, 177(7), 1915-1932.e16
17. Tikhonova AN, et al. (2019) The bone marrow microenvironment at single-cell resolution. Nature, 569 (7755), 222-228
18. Bandyopadhyay S et al. (2024) Mapping the cellular biogeography of human bone marrow niches using single-cell transcriptomics and proteomic imaging. Cell, 187(12), 3120
19. Konopleva M, et al. (2002) Stromal cells prevent apoptosis of AML cells by up-regulation of anti-apoptotic proteins. Leukemia, 16(9), 1713-1724
20. Zeng Z, et al. (2009) Targeting the leukemia microenvironment by CXCR4 inhibition overcomes resistance to kinase inhibitors and chemotherapy in AML. Blood, 113(24), 6215-6224
21. Nervi B, et al. (2011) CXCR4 antagonists: targeting the microenvironment to treat leukemia and lymphoma. Nat Rev Clin Oncol, 8(9), 457-466
22. Matsunaga T, et al. (2003) Interaction between leukemic-cell VLA-4 and stromal fibronectin is a decisive factor for minimal residual disease of acute myelogenous leukemia. Nat Med, 9(9), 1158-1165
23. Jin L, et al. (2006) Targeting of CD44 eradicates human acute myeloid leukemic stem cells. Nat Med, 12(10), 1167-1174
24. Wang Y, et al. (2010) The Wnt/β-catenin pathway is required for the development of leukemia stem cells in AML. Science, 327(5973), 1650-1653
25. Zhao C, et al. (2009) Hedgehog signalling is essential for maintenance of cancer stem cells in myeloid leukaemia. Nature, 458(7239), 776-779
26. Suzuki-Inoue K, et al. (2010) Essential in vivo roles of the C-type lectin receptor CLEC2: embryonic/neonatal lethality of CLEC2-deficient mice by blood/lymphatic misconnections and impaired thrombus formation of CLEC2-deficient platelets. J Biol Chem, 285(32), 24494-24507
27. Suzuki-Inoue K. (2019) Platelets and cancer-associated thrombosis: focusing on the platelet activation receptor CLEC-2 and podoplanin. Blood, 134(22), 1912-1918
28. Acton SE, et al. (2012) Podoplanin-rich stromal networks induce dendritic cell motility via activation of the C-type lectin receptor CLEC2. Immunity, 37(2), 276-289
29. Malhotra D, et al. (2012) Transcriptional profiling of stroma from inflamed and resting lymph nodes defines immunological hallmarks. Nat Immunol, 13(5), 499-510
30. Nakamura-Ishizu A, et al. (2015) CLEC-2 in megakaryocytes is critical for maintenance of hematopoietic stem cells in the bone marrow. J Exp Med, 212(12), 2133-46
31. Asada N, et al. (2017) Differential cytokine contributions of perivascular haematopoietic stem cell niches. Nat Cell Biol, 19(3), 214-223
32. Kumode T, et al. (2022) High expression of C-type-lectin-like-2 identifies a subset of human hematopoietic stem cells with megakaryocytic bias. Int J Hematol, 115(3), 310-321
33. Omatsu Y, et al. (2010) The essential functions of adipo-osteogenic progenitors as the hematopoietic stem and progenitor cell niche. Cell Stem Cell, 7(4): 472–484
34. Séverin S, et al. (2011) Syk-dependent phosphorylation of CLEC-2: a novel mechanism of hem-immunoreceptor tyrosine-based activation motif signaling. J Biol Chem, 286(6), 4107-4116
35. Finney BA, et al. (2012) CLEC-2 and Syk in the megakaryocytic/platelet lineage are essential for development. Blood, 119(7), 1747-56